Paper No.
5855

NACE INTERNATIONAL CORROSION 2015 CONFERENCE & EXPO

The Likelihood of Localized Corrosion in an H_2S / CO_2 Environment

Bruce Brown
Institute for Corrosion and Multiphase Technology
Department of Chemical & Biomolecular Engineering
Ohio University
342 W. State St.
Athens, OH 45701
U.S.A.

ABSTRACT

Understanding the mechanisms that lead to localized corrosion in oil and gas pipeline is of great interest to corrosion engineers worldwide. In a research program which examined corrosion under slightly sour conditions due to an H_2S/CO_2 environment, experimental studies were carried out to identify the environmental parameters with the most influence on the likelihood of localized corrosion. Observations of localized corrosion that occurred in slightly sour conditions in a large scale flow loop under single phase and multiphase flow were used to develop a better understanding of how bulk solution conditions can affect the growth of the corrosion product layers, over time, and their relationship to localized corrosion. It was shown that the solution bulk pH, ionic strength, and concentrations of carbonate and sulfide species are the major factors related to development of localized corrosion in a slightly sour environment. The experimental data was then analyzed and used to develop a correlation to relate these parameters to the likelihood of localized corrosion.

Key words: localized corrosion, sour corrosion, pitting, hydrogen sulfide, carbon dioxide, iron sulfide, iron carbonate, ionic strength, pitting ratio, pH, chloride

INTRODUCTION

Localized corrosion in its most extreme form is defined as a non-uniform loss of metal from the internal pipe wall of an upstream oil and gas pipeline which leads to a loss of containment. Pipelines designed to withstand 50 years of operation under the worst case general corrosion rate may fail after a few months of operation due to localized corrosion. Loss of containment from a pipeline failure is a costly event as it would cause an emergency shutdown in the production of oil and/or gas, an emergency repair of the pipeline, and probably an environmental clean-up at the leak site. In an effort to minimize pipeline failures and loss of containment, companies around the world in the oil and gas industry sponsor research programs focused on better prediction and mitigation methods for localized corrosion.

This report uses data and conclusions from the author's PhD dissertation entitled "The Influence of Sulfides on Localized Corrosion of Mild Steel"[1] to highlight experiments which delineate the effect of

multiple parameters on the rate of localized corrosion over a wide range of conditions for an $H_2S/CO_2/H_2O$/Fe system. In the analysis of experimental data to develop a correlation to predict the likelihood of localized corrosion in sour systems, the key parameters of interest in the development of a mechanistic model for localized corrosion are identified.

EXPERIMENTAL PROCEDURE

Large Scale Flow Loop

A large scale, 2000 liter, H_2S flow loop was used for all experiments to provide a two-phase water/gas environment including provisions for multiphase flow and single phase flow test sections in a 10.1 cm ID pipeline. This ensures that testing is conducted in multiphase flow regimes that can be scaled up to similar to conditions observed in working pipelines. The solution temperature, pH, flow rates, and partial pressures of both gases were controlled during testing. The full description of the large scale H_2S system was previously published[2] during the early stages of testing and a full report[3] is available which fully describes the large-scale, multiphase flow loop used for the study of corrosion in sour gas environments.

For corrosion measurements, the H_2S flow loop holds 7 weight (mass) loss (WL) specimens in three test sections: one single phase test section and two test sections for bottom of the line multiphase testing. The API 5L X65 WL specimens used were 1.25" (31.75 mm) in diameter and 0.25" (6.35 mm) thick. The WL specimens were installed and removed with the environmental conditions of each test maintained, meaning that the H_2S flow loop is at the proper temperature, pCO_2, and pH_2S as the WL specimens were inserted and removed from the experiment. The WL specimens were flush mounted with the internal pipe diameter to present an environment similar to a continuous pipe surface. Safety procedures are strictly adhered to when working in a system containing any amount of H_2S.

Pitting Ratio

The definition for pitting ratio used in these experiments is shown in Equation (1) as the ratio of the deepest localized corrosion location found on the surface of the specimen after layer removal to the general corrosion rate calculated by the weight loss method.

Pitting Ratio = [Penetration Rate (mm/yr)] / [General Corrosion Rate (mm/yr)] (1)

This equation is flawed as it does not take into account the surface area affected by localized corrosion. Therefore, documentation of visual observations for each specimen plays a significant role in determination of localized corrosion. If the "localized corrosion" covers more than 50% of the specimen surface and the pitting ratio ≅ 1, then it can be assumed that the "localized" corrosion found is just the initiation points of general corrosion on the metal surface. If it is assumed that the pitting ratio is between 3 and 5, the amount of "localized" corrosion could not cover a significant percentage of the specimen surface and would be considered to have a 50% chance of becoming a more significant localized corrosion. However, if the pitting ratio is greater than 5 the penetration rate exceeds the general corrosion rate by so much that it must be "localized" corrosion.[1]

RESULTS AND DISCUSSION

The experimental conditions used in this study focused on a "slightly sour" corrosion environment with CO_2 present and were chosen to develop only partially protective corrosion product layers. The partial pressures, temperatures, and pH were defined such that some experimental conditions tested would have the carbonic acid concentration dominant whereas some conditions tested would have the aqueous H_2S concentration dominant. The ranges of parameters studied are listed in Table 1. It should

be noted that there are a limited number of large scale test facilities for sour corrosion research related to internal pipeline corrosion available worldwide. Due to the nature of testing with a hazardous gas, most of the studies referred to in the literature are limited to autoclaves which are unable to produce the correct physics of the flow for the simulation of corrosion in multiphase slug flow.

Table 1
List of Parameters Tested in the Large Scale H_2S Flow Loop

Parameter	Description
Total pressure	3 bar, 8 bar
Temperature	25°C, 40°C, 60°C
Test duration	10, 20, 30 days or 7, 14, 21 days
Electrolyte	1 wt % NaCl, 10 wt% NaCl
pH	4.5, 5.0, 6.0
Superficial Liquid Velocity (V_{sl})	0.1 m/s, 1 m/s
Superficial Gas Velocity (V_{sg})	0 m/s, 1 m/s, 3 m/s
pCO_2	2.7, 2.9, 7.7 bar
pH_2S	0.25, 0.1, 1, 1.2, 4, 10, 100 mbar

Relationship of Parameters to the Likelihood of Localized Corrosion

Relationship of Localized Corrosion to Saturation Values

The calculated values for saturation of iron carbonate and iron sulfide can be good indicators of when corrosion product layers are likely to form, but are not directly related to the localized corrosion phenomenon since many factors are used in the calculation and each factor has its own direct relationship to the type of layer developed. The saturation values for iron carbonate, $S(FeCO_3)$, and iron sulfide, S(FeS), are calculated as shown in Equation (2) and Equation (3):

$$S(FeCO_3) = \frac{[Fe^{2+}][CO_3^{2-}]}{K_{sp}(FeCO_3)} \quad (2)$$

$$S(FeS) = \frac{[Fe^{2+}][HS^-]}{[H^+]K_{sp}(FeS)} \quad (3)$$

If the saturation values are greater than 1 there is an indirect relationship to localized corrosion, because precipitation of iron sulfide and/or iron carbonate is possible which can lead to the development of galvanic cells under the right environmental conditions. To capture this mechanism for the likelihood of localized corrosion, an interaction parameter was defined as the log of the product of the saturation values: log(S(FeS)*$S(FeCO_3)$). This interaction parameter will be negative when the system is undersaturated with respect to iron carbonate and/or iron sulfide, but will be positive when both are above saturation (supersaturated) and will increase in magnitude when the values are both highly supersaturated. The interaction parameter is an indication of the scaling tendency of the system and observations have shown more localized corrosion occurs due to imperfections in the growth of the corrosion product layer.

Experiment at 60°C, pCO_2 = 7.7 bar, pH_2S = 10 mbar, pH 6.0, 1 wt% NaCl

For the experiment at 60°C, pCO_2 = 7.7 bar, pH_2S = 10 mbar, pH 6.0, 1 wt% NaCl, the average saturation value for iron sulfide was near 150 while the average iron carbonate saturation value was just above 10; therefore, one would expect the corrosion product to be highly dominated by iron sulfide. The operating parameters for this experiment are shown in Table 2.

Table 2
Controlled Parameters for S(FeS) ≈ 10[S($FeCO_3$)]

Parameter	Description
Equipment	H_2S Flow Loop
Test duration	25 days
Temperature	59.8 ± 0.8 °C
pCO_2	7.7 ± 0.9 bar
pH_2S	10 ± 1.6 mbar
pH	6.0 ± 0.1
Electrolyte	1 wt% NaCl
Ionic strength	0.28± 0.02
[Fe^{2+}] (ppm)	2.3 ± 1.2
S($FeCO_3$)	13 ± 9
S(FeS)	151 ± 111
S(FeS)/S($FeCO_3$)	11.7 ± 0.5

[#](avg ± std deviation)

Observations of WL specimens from each time exposure to single phase and multiphase flow conditions are shown in Figure 1. As expected in an H_2S dominated environment, the corrosion product was black and fully covered the metal surface. EDS analysis of the corrosion product layer shows iron sulfide dominant on the bulk solution side (assumed to be mackinawite), but the presence of iron carbonate was detected near the metal surface.[1]

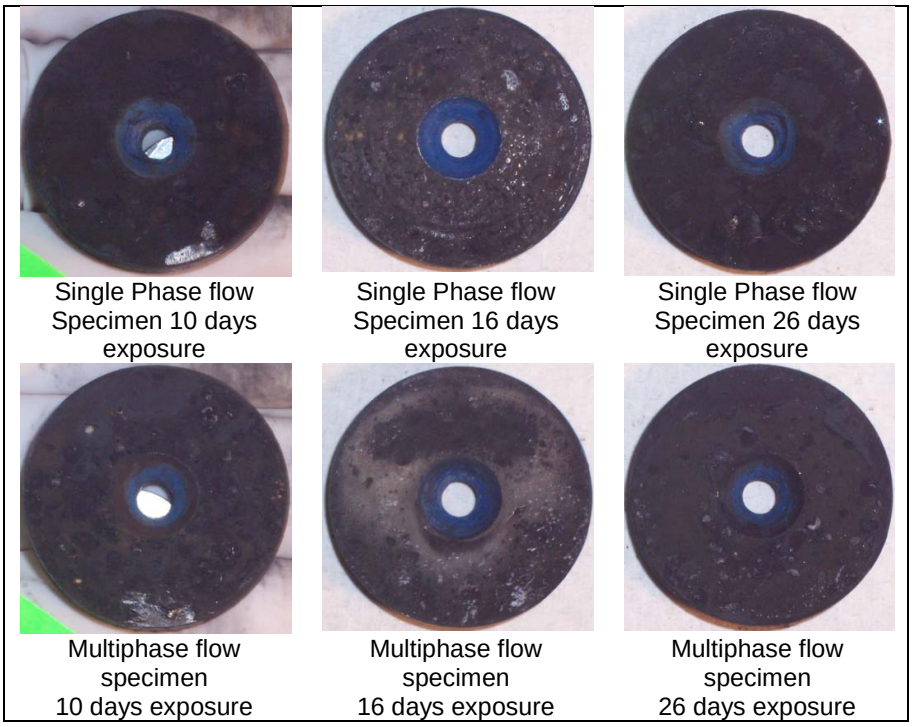

Figure 1: Visual examination of WL specimens as removed from experiment. (60°C, P_{total} = 8 bar, 10 mbar ± 1 mbar pH_2S [1000ppm], 1 wt% NaCl)

All WL specimens from this experiment show surface variations of 10 μm to 40 μm due to corrosion, but only the WL specimen exposed for the first 10 days of the experiment in multiphase flow could be defined as having localized corrosion with a maximum pit depth measured from cross-sectional analysis of 340 μm (Figure 2). The 60°C, pCO_2 = 7.7 bar, pH_2S = 10 mbar, pH 6.0, 1 wt% NaCl data set is assumed to have a 50% chance for localized corrosion since the pitting ratio is greater than 3, but less than 5 (pitting ratio = 4.1) as defined by Equation (1).

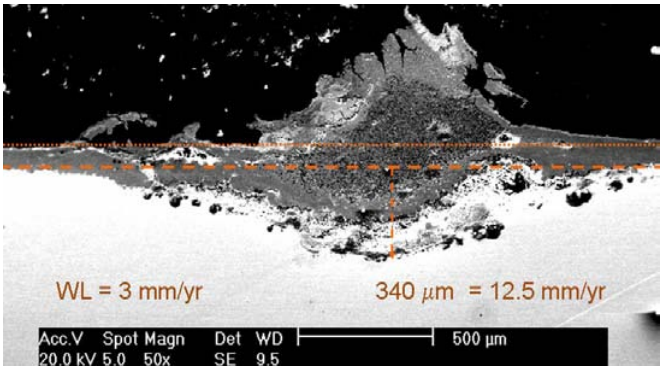

Figure 2: Cross section with calculation of general corrosion rate vs. localized corrosion rate for multiphase flow specimen after 10 days exposure. (60°C, P_{total} = 8 bar, 10 mbar ± 1 mbar pH_2S [1000ppm], 1 wt% NaCl)

Experiment at 60°C, pCO_2 = 7.7 bar, pH_2S = 0.1 mbar, pH 6.0, 1 wt% NaCl

For the experiment at 60°C, pCO_2 = 7.7 bar, pH_2S = 0.1 mbar, pH 6.0, 1 wt% NaCl, the average saturation value for iron sulfide was less than half of the average iron carbonate saturation value during this experiment; therefore, one would expect the surface layers to be slightly more influenced by iron carbonate precipitation than by iron sulfide precipitation. The operating parameters for this experiment are shown in Table 3.

Table 3
Controlled Parameters for S(FeS) ≈ (15%)[S($FeCO_3$)].

Parameter	Description
Equipment	H_2S Flow Loop
Test duration	30 days
Temperature	60.2 ± 0.6 °C
pCO_2	7.7 ± 0.1 bar
pH_2S	0.12 ± 0.04 mbar
pH	6.0 ± 0.1
Electrolyte	1 wt% NaCl
Ionic strength	0.254 ± 0.004
[Fe^{2+}] (ppm)	4.3 ± 0.6
S($FeCO_3$)	15.2 ± 3.2
S(FeS)	2.2 ± 1.2
S(FeS)/S($FeCO_3$)	0.14 ± 0.06

[#](avg ± std deviation)

Observations of WL specimens from three time exposures (10, 20, & 30 days) show that the corrosion product layer was thin with a more uniform coverage developed after the full 30 day exposure (Figure 3). The multiphase flow specimen and single phase flow specimen seemed to have similar surface coverage by corrosion product, although the measured corrosion rate for single phase was much less than for multiphase flow.

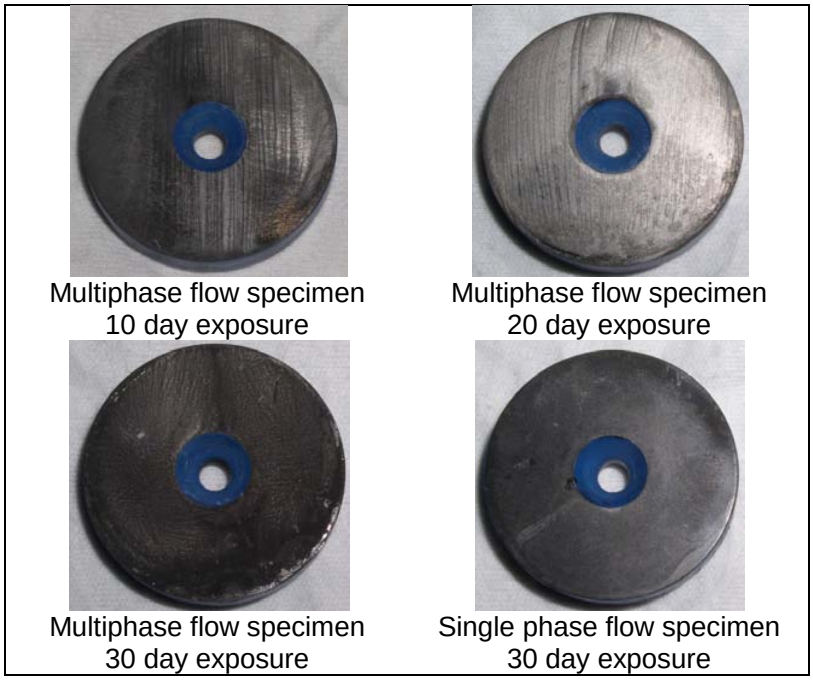

Figure 3: Visual examination of WL specimens as removed from experiment. (60°C, 7.7 bar CO_2, pH 6.0, pH_2S = 0.12 mbar ± 0.04 mbar)

Cross-sectional analysis on the multiphase specimen after 30 days shows a uniform corrosion product layer with a thickness of 28 to 30 μm (Figure 4).

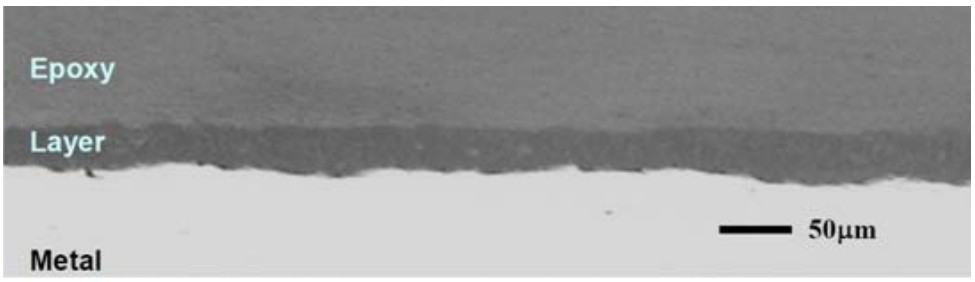

Figure 4: Cross sectional analysis of multiphase WL specimen of API 5L X65 after 30 day exposure. Corrosion product is approximately 28 to 30 μm thick. (100X metallurgical microscope, 60°C, 7.7 bar CO_2, pH_2S = 0.12 mbar ± 0.04 mbar).

Although the corrosion product layer developed under experimental conditions at 60°C, pCO_2 = 7.7 bar, pH_2S = 0.1 mbar, pH 6.0, 1 wt% NaCl retards the corrosion as related to the same corrosive environment without the presence of H_2S, only a few microns in depth was required to retard corrosion. This very thin layer also seems to show that it may be influenced by flow as indicated by the lines and directional structure of the corrosion product in the images of the multiphase WL specimens (Figure 3). This is an example of a corrosion product that has been thought to be amorphous in nature as no crystalline features are visible even at a high magnification. EDS analysis shows iron sulfide was dominant in the corrosion product layer with no indication of a carbonate component.[1] It is assumed

that the lack of an iron carbonate component in the corrosion product layer for this experiment led to a general corrosion with a thin corrosion product layer of iron sulfide and no observable localized corrosion.

Relationship of Localized Corrosion to Ionic strength

A change in ionic strength is understood to have an effect on iron carbonate precipitation, but little is known about its effect on iron sulfide corrosion products. In the current experiments, an increase in the ionic strength of the solution (by an increase in sodium chloride concentration) from 0.26 to 1.8 did not have much effect on the general corrosion rate, but was found to increase metal loss underneath the corrosion product layer indicating an increased likelihood toward localized corrosion. When considering a porous corrosion product layer with a mixed iron sulfide / iron carbonate composition, an increase in the ionic strength of the solution decreases the saturation value for iron carbonate[4] which would lead to a decrease of iron carbonate precipitation within the corrosion product layer and near the metal surface, thus allowing more metal loss under the corrosion product layer (undermining). Ionic strength is thought to be a significant indicator for the likelihood of localized corrosion.

Experiment at 60°C, pCO_2 = 7.7 bar, pH_2S = 10 mbar, pH 6.0, 10 wt% NaCl

For the experiment at 60°C, pCO_2 = 7.7 bar, pH_2S = 10 mbar, pH 6.0, 10 wt% NaCl, the concentration of sodium chloride was 10 wt% in solution, but the average partial pressure of H_2S was 10 mbar (Table 4). This experiment is complementary to the previous two experiments shown to observe the effect of an increase in the ionic strength (as compared to Table 2) or an increase in pH_2S (as compared to Table 3) as related to the likelihood for localized corrosion in a sour system.

Table 4
Controlled Parameters for High Sodium Chloride Test at 10 mbar pH_2S.

Parameter	Description
Equipment	H_2S Flow Loop
Test duration	30 days
Temperature	60.1 ± 1.0 °C
pCO_2	7.7 ± 0.2 bar
pH_2S	10 ± 1 mbar
pH	6.0 ± 0.2
Electrolyte	10 wt% NaCl
Ionic strength	1.9 ± 0.07
$[Fe^{2+}]$ (ppm)	2.5 ± 0.5
S($FeCO_3$)	7.7 ± 5.9
S(FeS)	32.8 ± 25.6
S(FeS)/S($FeCO_3$)	4.2 ± 0.1

[#](avg ± std deviation)

The effect of the increase in sodium chloride concentration was seen on the first WL specimen removed. After 10 days exposure time in multiphase flow, the WL specimen in Figure 5 shows localized corrosion through a comparison with and without the corrosion product layer as taken by profilometer measurements. With the corrosion product layer in place (left image), the variation of the surface topography is extreme as compared to all other WL specimens with a 1.7 mm peak of “debris” located on the specimen surface. After removal of the corrosion product by Clarke solution[5] (right image), the general corrosion rate was calculated at 2.7 mm/yr and, through profilometer analysis, the maximum depth of attack was measured to be 0.36 mm or 14.1 mm/yr. This is considered to be localized corrosion since the pitting ratio is greater than 5 (pitting ratio = 5.3) as defined by Equation (1).

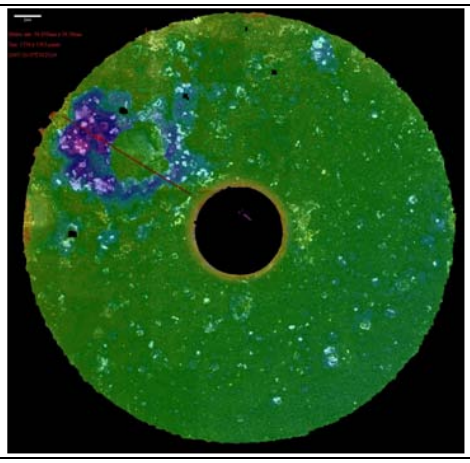

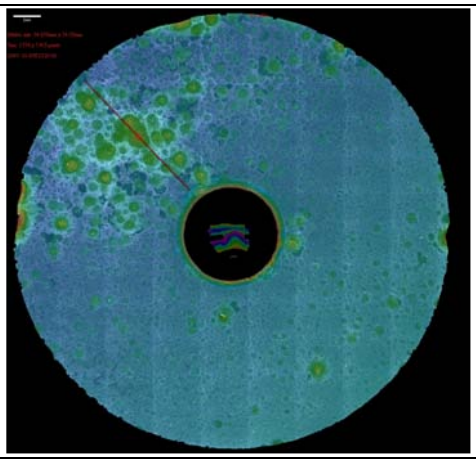

With corrosion product layer intact	**After corrosion product layer removed**
Maximum peak of topography: 1.7 mm	0.63g layer weight loss

Figure 5: API 5L X65 specimen recovered from multiphase flow test section after 10 days at 60°C, pCO_2 = 7.7 bar, pH 6.0, 10 mbar H_2S, 10 wt% NaCl

The three experiments reviewed in this section show that an increase in pH_2S from 1 mbar to 10 mbar slightly increased the likelihood for localized corrosion in a sour system, but an increase in both pH_2S and ionic strength definitely increased the likelihood of localized corrosion in a sour system.

Relationship of Localized Corrosion to Solution pH

The pH of the solution has a direct influence on the development of the corrosion product layer and therefore has a strong influence on the likelihood for localized corrosion. At pH 4 in an H_2S/CO_2 system, iron carbonate is always under-saturated, so localized corrosion would have to be related to the thickness of the developed iron sulfide layer and the probability of localized corrosion is low. At pH 6 and above in an H_2S/CO_2 system, the iron sulfide saturation value can become quite high with just a small concentration of ferrous ions, so precipitation of iron sulfide on top of the corrosion product layer was always observed. Any ferrous ions that migrate through the corrosion product layer at pH 6 will immediately react with the available sulfides to become iron sulfide, *i.e.*, "fluffy" mackinawite.[6] At pH 5 in an H_2S/CO_2 system, the corrosion product layer developed does not have much of a precipitation layer on top of the initial corrosion product layer and the localized corrosion locations underneath the corrosion product layer are usually filled, not empty.

Comparison of the general and localized corrosion rates measured during this study are shown in Figure 6, Figure 7 and Figure 8. By breaking down the large data set of experiments into exposures by time, flow regime and bulk pH, some characteristics of the iron sulfide layer with respect to general and localized corrosion are revealed. These figures provide the comparison of data at 1 week, 2 weeks and 3 weeks exposure time, respectively, with each figure providing a separation of corrosion rates for the a) single phase (SP) flow and b) multiphase (MP) flow regimes.

After 1 week exposure time, the iron sulfide corrosion product layer has already covered the surface of the mild steel. From Figure 6, it can be seen that the corrosion rate for pH 5.0 is negligible, indicating that the initial corrosion product layer formed for this experiment is still protective while localized corrosion has already initiated at pH 4.5 and pH 6.0.

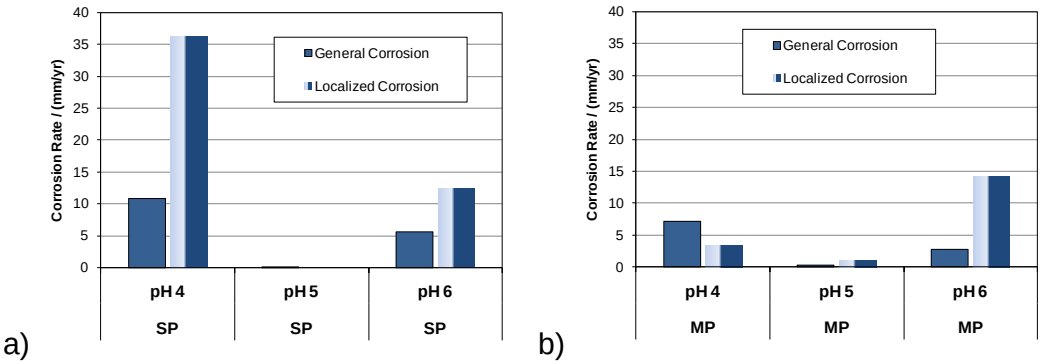

Figure 6: Comparison of general and localized corrosion for single phase flow (a) and multiphase flow (b) at pH 4.5, pH 5.0, & pH 6.0 for a 1 week exposure (60°C, pCO_2 = 7.7 bar, pH_2S = 10 mbar, 10 wt.% NaCl).

For the WL specimens exposed for 2 weeks, the flow regime has a much greater effect on the general corrosion rate observed at pH 4.5 and pH 5.0. By comparison of Figure 7a) to Figure 7b), the corrosion product formed at pH 4.5 and pH 5.0 was not a good mass transfer barrier and may have promoted an increased corrosion rate since there is such a large difference observed. Neither the general or localized corrosion rates at pH 6.0 were influenced by the flow regime.

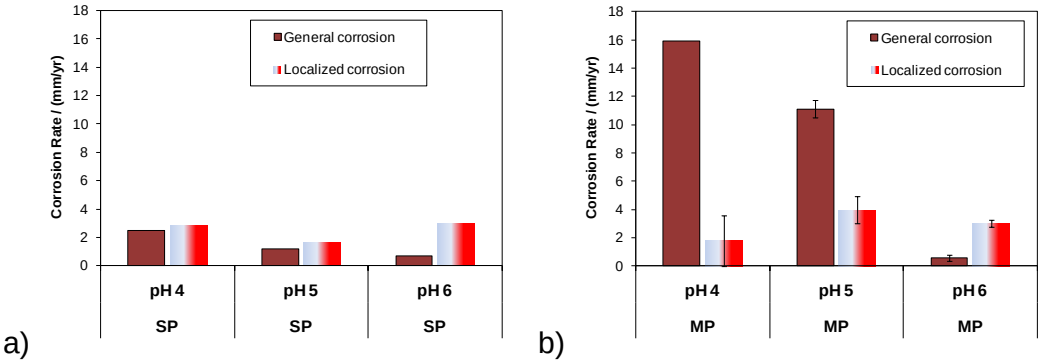

Figure 7: Comparison of general and localized corrosion for single phase flow (a) and multiphase flow (b) at pH 4.5, pH 5.0 & pH 6.0 for a 2 week exposure (60°C, pCO_2 = 7.7 bar, pH_2S = 10 mbar, 10 wt.% NaCl).

After exposure for 3 weeks, corrosion rate comparison in Figure 8 shows high general corrosion rates at pH 4.5 and pH 5.0 which appear to limit the likelihood of localized corrosion. When localized corrosion occurred at pH 5.0, it was the highest recorded localized loss of material for this entire test series (Figure 9). Localized corrosion at pH 6.0 was consistent and similar between the different flow regimes.

The amount and depth of localized corrosion is higher in a pH 6 solution than for either pH 5 or pH 4 solutions, so a dramatic increase in the likelihood for localized corrosion is shown to be related to precipitation on top of the initial corrosion product layer.

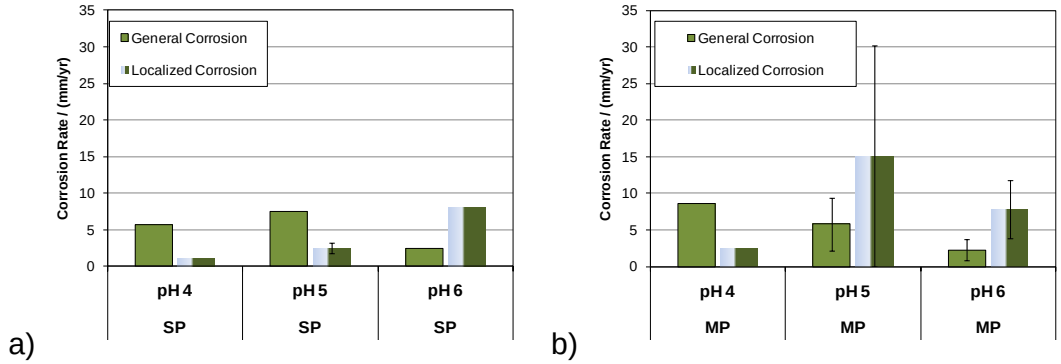

Figure 8: Comparison of general and localized corrosion for single phase flow (a) and multiphase flow (b) at pH 4.5, pH 5.0 & pH 6.0 for a 3 week exposure (60°C, pCO_2 = 7.7 bar, pH_2S = 10 mbar, 10 wt.% NaCl).

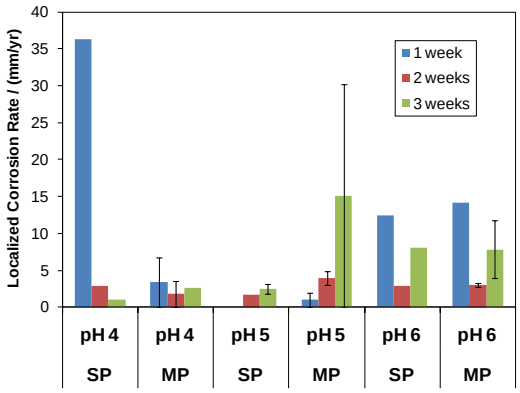

Figure 9: Localized corrosion rates measured by profilometer for testing conducted at pH 4.5, pH 5.0 & pH 6.0 in the multi-week experiment (60°C, pCO_2 = 7.7 bar, pH_2S = 10 mbar, 10 wt.% NaCl).

Review of the two WL specimens with the largest penetration rates in Figure 9 provides supporting evidence for the relationship of corrosion product layer to localized corrosion.

At pH 4.5, an SEM image of failure locations show a corrosion product layer that has collapsed and been swept away by the flow (left side of Figure 10). When the corrosion product was removed, this specimen did show multiple locations of a pitting type corrosion with an average depth of 150μm (8 mm/yr penetration rate) which were not considered localized corrosion as the general corrosion rate was measured at 10.8 mm/yr. Only one location, shown on the right side of Figure 10, was found with a depth large enough to be defined as localized corrosion. This is a 681μm pit which is calculated to have a 36.3 mm/yr penetration rate. Consequently, this is considered localized corrosion.

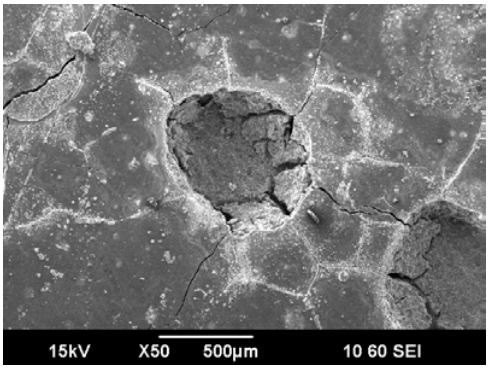

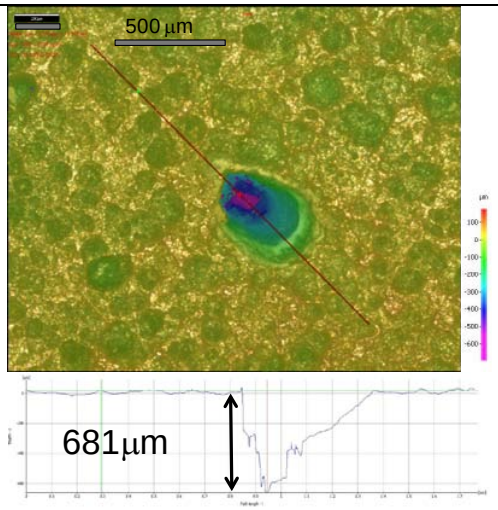

Multiphase 7 days with corrosion product layer	Multiphase 7 days without corrosion product.

Figure 10: 60°C, pCO_2 = 7.7 bar, pH_2S = 10 mbar, 10 wt% NaCl, 7 days exposure at pH 4.5. Penetration corrosion rate 36.3 mm/yr, general corrosion rate 10.8 mm/yr.

For the localized corrosion measured at pH 5, the specimen image is shown in Figure 11. This specimen has a 0.5" (1.3 cm) area of localized corrosion that was too large to view in a single SEM image, so the image of the entire gold-coated cross sectional specimen was captured by a profilometer. Note the three localized areas of attack on the specimen surface. The one to the farthest right still contains the corrosion product layer and has a measured depth of 1.8 mm for a 30 mm/yr penetration rate. This WL specimen had a weight loss of 0.78 grams (including the corrosion product) for a general corrosion rate of 2.2 mm/yr. It can be assumed that the entire weight loss of this specimen was related to localized corrosion.

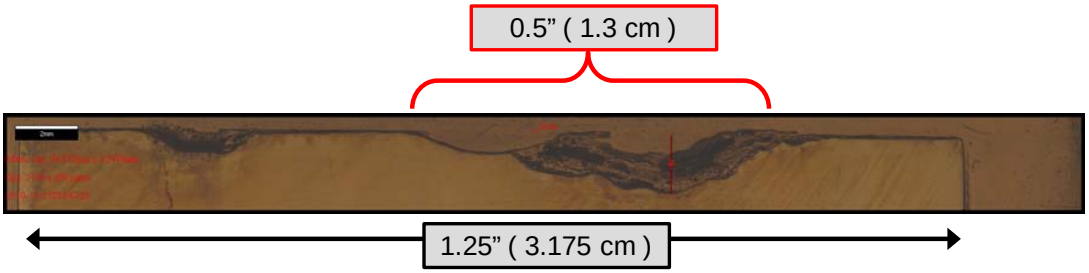

Figure 11: IFM image of the whole cross-section of the multiphase specimen taken at 22 days. Multiphase WL specimen taken from 60°C, pH 5, pCO_2 = 7.7 bar, pH_2S = 10 mbar, 10 wt% NaCl.

An interesting feature of the corrosion product layer shown in Figure 11 is the thin layer of corrosion product (iron sulfide) covering the flat portions of the left, right, and center portions of specimen thought to represent the original metal surface, and covering the 4.5 mm wide pit in the center of the image. This pit may have started at the same time as the one taking up the right half of the image, but through some mechanism lost its partial layer coverage and when subjected to the bulk conditions it developed the thin layer of corrosion product that provided some limitation to the corrosion reaction and the pit propagation stopped. This may be a case where one of two adjacent pits became dominant.

This series of experiments provide proof that the solution pH is a strong indicator for the prediction of localized corrosion as it is directly related to the corrosion product layer that will form on the metal surface.

Relationship of Localized Corrosion to a Decrease in pCO_2

A decrease in partial pressure of CO_2 would be expected to decrease the amount of [H_2CO_3] and [HCO_3^-] available for diffusion through the corrosion product layer which would change the water chemistry conditions that could occur within the corrosion product layer. In the comparison between experiments, a decrease in the partial pressure of CO_2 seemed to increase the likelihood of developing localized corrosion, but also included an increase in the solution pH.

Localized corrosion for a specimen exposed to conditions with 2.7 bar pCO_2, 10 mbar pH_2S, 60°C, and pH 6 for 14 days was 12.8 mm/yr with a general corrosion rate of 0.75 mm/yr (Figure 12) for a pitting ratio of 17. An iron carbonate layer (dark gray) was found under the iron sulfide layer (light gray) as determined by SEM/EDS analysis (left side of Figure 12).

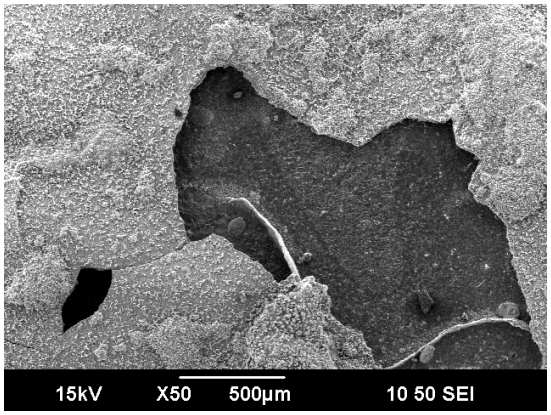

SEM with corrosion product layer

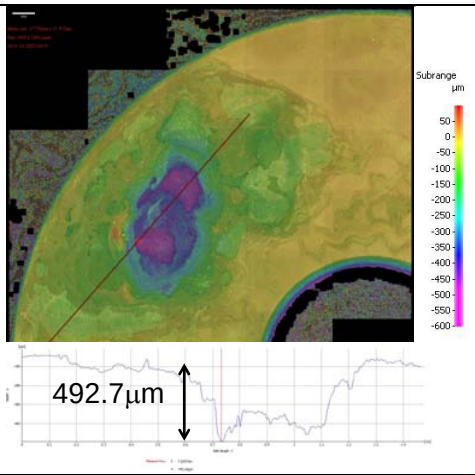

Profilometer without corrosion product layer

Figure 12: SEM and profilometer analysis of specimen showing the type of corrosion product layer and depth of localized corrosion. Multiphase flow WL specimen 14 days, 60°C, pH 6, pCO_2 = 2.7 bar, pH_2S = 10 mbar, 1 wt% NaCl

Table 5
Environmental conditions for eight experiments at 1 wt% NaCl that involve a change in pCO_2 for comparison.

pCO_2 (bar)	pH_2S (bar)	Temp (°C)	pH	Localized Corrosion?	$FeCO_3$ Crystal structure observed?
7.7	0.0012	60	6	Yes (PR ≥ 5)	No
7.7	0.010	60	6	Maybe (3 ≤ PR < 5)	Yes
7.7	0.001	60	5	No (PR < 3)	No
7.7	0.010	60	5	No (PR < 3)	Yes
2.7	0.010	60	6	Yes (PR ≥ 5)	Yes
2.9	0.004	40	5	Yes (PR ≥ 5)	No
2.8	0.10	25	5	No (PR < 3)	No
2.8	0.13	40	5	Maybe (3 ≤ PR < 5)	Yes

The presence of iron carbonate as a recognizable species in the corrosion product layer was thought to have some relationship to the likelihood of localized corrosion, but a simple comparison over the 8 experiments in Table 5 does not show any obvious correlation between the visual presence of iron carbonate and measured localized corrosion. This is an indication that the use of the solution

concentrations of $[H_2CO_3]+[HCO_3^-]$ and $[H_2S]+[HS^-]$ has more significance than the partial pressures of the acid gases since these values will also be related to the temperature and pH of the environment.

Prediction Model for Localized Corrosion

A solution for the likelihood of localized corrosion was determined using the technique of Gaussian elimination, shown in Equation (4). The full data set is comprised of 78 WL specimens which determine the likelihood for localized corrosion for the 11 environmental conditions tested. This set of equations was solved according to:

$$a_1 x_1 + a_2 x_2 + \cdots a_n x_n = p_1 \quad (4)$$

where a = parameter coefficient,
x = parameter value, and
p is the unique solution.

The parameters used for the solution of Equation (4) are based on the chemical, electrochemical, and precipitation reactions at each experimental condition tested with focus on elucidation of possible interactions between parameters. The set of equations used for this correlation can be found in the 2003 report by Nordsveen, et al.[4] Results are shown in Table 6.

Table 6
Definition of parameters used for correlation with calculated coefficients.

Parameter Title	Coefficient (*a*)	Sensitivity	Parameter definition (*x*)
Temperature	-1.94	± 0.016 (± 1.1%)	T_K
pH	59.45	± 1.1 (± 1.5%)	pH
Carbonate concentration	-99.25	± 2.5 (± 2.5 %)	$\log([H_2CO_3]+[HCO_3^-])$
Sulfide concentration	-31.46	± 1.6 (± 5 %)	$\log([H_2S]+[HS^-])$
Ionic strength	25.65	± 2.6 (± 10 %)	I
Iron sulfide saturation	0.11	- - -	S(FeS)
Iron carbonate saturation	0.32	- - -	$S(FeCO_3)$
Interaction of saturation values	12.71	± 2.5 (± 20 %)	$\log(S(FeS)*S(FeCO_3))$

Five of the parameters used in data correlation (T_K, pH, I, S(FeS), $S(FeCO_3)$) were reviewed directly in the research as each play a role in defining the environmental conditions. An indirect effect of pCO_2 and pH_2S is also expected, so the species in solution that can directly or indirectly provide hydrogen ions for the corrosion reaction were used ($[H_2CO_3]$, $[HCO_3^-]$, $[H_2S]$, $[HS^-]$). Because the equilibrium constants relating to carbonic acid, bicarbonate, aqueous hydrogen sulfide, and bisulfide are an exponential function of temperature, the base 10 logarithm of these values are used as the linear transform of the data in order to fit them in the set of linear equations. An interaction parameter was also necessary to provide an indication of corrosion product layer formation and was provided by using the base 10 logarithm of the product of saturation values. This value will be positive when both saturation values are above 1 (supersaturated conditions for both species), but negative when the

system is not dominated by either iron sulfide or iron carbonate precipitation (undersaturated for both species). Direct comparison of the likelihood values calculated can be seen in Figure 13 for the 11 datasets. The raw data of pitting ratio for each of the 78 WL specimens is also shown in comparison to the measured and calculated likelihood for localized corrosion in Figure 14.

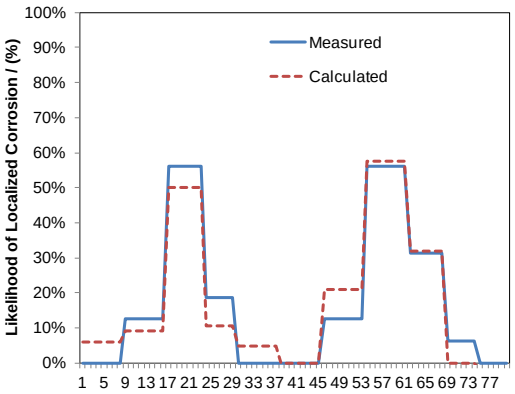

Figure 13: Direct comparison of measured and calculated likelihood for localized corrosion under the tested conditions.

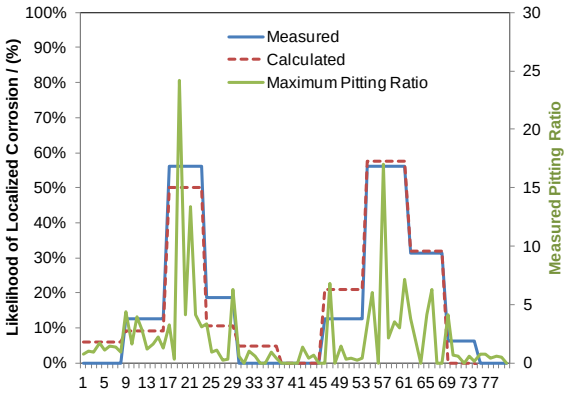

Figure 14: Comparison of the measured maximum pitting ratio for 78 WL specimens to the measured and calculated values for likelihood of localized corrosion.

In order to identify which variables are more important in the calculation of the likelihood of localized corrosion, a qualitative review of the parameters was done to determine their sensitivity to change. The sensitivity of each of the parametric coefficients in Table 6 was tested through comparison of the calculated value to the measured value of the likelihood of localized corrosion while varying that specific parameter. The maximum difference between the measured and calculated values for the likelihood of localized corrosion in Figure 13 is less than 9%. In order to determine a value for sensitivity, the maximum difference was not allowed to exceed 15% while changing each specific variable. The results in Table 6 are shown as an uncertainty and a percent change for each coefficient.

A comparison of the coefficient sensitivity values in Table 6 shows which parameters are more sensitive to change. The model is most sensitive to changes in the coefficients for temperature and pH, where changes from 1% to 2% change the output of the model by more than 15%. The coefficients for the concentrations of carbonates and sulfides in solution affect the outcome of the model if they are varied by 2.5% to 5%, which shows that these variables are also highly significant in the calculation of the model. The values of uncertainty for iron carbonate saturation and iron sulfide saturation coefficients were not calculated because they are used in the interaction parameter and would not be varied independently. The coefficient for the interaction of the saturation values is the least sensitive parameter, which is an indication that the degree of saturation is not as important as having both iron carbonate and iron sulfide saturation in solution.

It must be understood that the form of Equation (4) does not have any intrinsic boundaries, so some must be imposed. Values calculated for the likelihood of localized corrosion are valid in the range from 0 to 100%. Magnitudes of calculated values that exceed this range, whether positive or negative, do not have any justifiable meaning and should be limited to these boundary values.

CONCLUSIONS

- Partial pressures of the acid gases (pCO_2 and pH_2S) are not good indicators for the likelihood of localized corrosion as the dissolution of both species are affected by temperature and solution pH. It was found that solution pH, ionic strength, and an interaction parameter of iron carbonate and iron sulfide saturation values provided the best indications for the likelihood of localized corrosion. No obvious correlation could be derived between the visual presence of iron carbonate in a mixed corrosion product layer and the probability of localized corrosion.

- In a series of experiments at 60°C, 7.7 bar pCO_2, 10 mbar pH_2S, 10 wt% NaCl, an increase in solution pH from pH 4.5 to pH 6.0 increased the frequency or likelihood of localized corrosion indicating that solution pH is a strong indicator for the prediction of localized corrosion as it is directly related to the corrosion product layer that will form on the metal surface.

- In a system with only general corrosion observed (60°C, 7.7 bar pCO_2, 1 mbar pH_2S, 1 wt % NaCl), localized corrosion occurred for similar conditions with an increased pH_2S (1 mbar vs. 10 mbar) and became more pronounced for similar conditions with an increase in the ionic strength (1 wt% NaCl vs. 10 wt% NaCl).

ACKNOWLEDGEMENTS

I would like to express my sincere gratitude to the faculty, staff, and researchers at the ICMT who have helped me to develop my current understanding of corrosion mechanisms in a sour environment (Dr. Srdjan Nešić, Dr. Marc Singer, Dr. Yoon-Seok Choi, Dr. David Young, Dr. Wei Sun, Dr. Kun-Lin John Lee, Stephen Smith, Yougui Zheng, and Ning Jing to name a few.) I would also like to acknowledge the industrial sponsors who have supported the Corrosion Center JIP over the period of this research (BG Group, BP, NALCO Champion, Chevron, Clariant Oil Services, ConocoPhillips, Encana, ENI S.P.A., ExxonMobil, MI-SWACO, Occidental Oil Company, Petrobras, PETRONAS, PTT, Saudi Aramco, INPEX Corporation, Total, TransCanada, and WGIM.)

REFERENCES

1. B. Brown. "The Influence of Sulfides on Localized Corrosion of Mild Steel." Electronic Dissertation. Ohio University, December 2013. *OhioLINK Electronic Theses and Dissertations Center*. https://etd.ohiolink.edu/.
2. B. Brown, A. Schubert, “The Design and Development of a Large-Scale Multiphase Flow Loop for the Study of Corrosion in Sour Gas Environments,” NACE Corrosion 2002, paper no. 02502.
3. B. Brown, “H_2S Multiphase Flow Loop: CO_2 Corrosion in the Presence of Trace Amounts of Hydrogen Sulfide,” Ohio University, MSChE Thesis, November 2004.
4. M. Nordsveen, S. Nešić, R. Nyborg, A. Stangeland, A Mechanistic Model for Carbon Dioxide Corrosion of Mild Steel in the Presence of Protective Iron Carbonate Layers – Part 1: Theory and Verification, Corrosion, May 2003, vol. 59, no. 5, pp 443 – 456.
5. ASTM G1 – 81, (Section 7),“ Standard Practice for Preparing, Cleaning, and Evaluating Corrosion Test Specimens,” Proceedings of the Symposium on Laboratory Corrosion Tests and Standards, G. S. Haynes, R. Balboian, editors, pp. 505-510, 1983.
6. S. N. Smith, B. Brown, W. Sun, “Corrosion at Higher H_2S Concentrations and Moderate Temperatures,” NACE Corrosion 2011, Paper No. 11081.